Enhancement of Ebola virus infection by seminal amyloid fibrils

Stephen M. Bart[a], Courtney Cohen[b], John M. Dye[b], James Shorter[c], and Paul Bates[a,1]

[a]Department of Microbiology, Perelman School of Medicine, University of Pennsylvania, Philadelphia, PA 19104; [b]Virology Division, United States Army Medical Research Institute of Infectious Diseases, Frederick, MD 21702; and [c]Department of Biochemistry and Biophysics, Perelman School of Medicine, University of Pennsylvania, Philadelphia, PA 19104

Edited by Peter Palese, Icahn School of Medicine at Mount Sinai, New York, NY, and approved May 29, 2018 (received for review December 14, 2017)

The 2014 western Africa Ebola virus (EBOV) epidemic was unprecedented in magnitude, infecting over 28,000 and causing over 11,000 deaths. During this outbreak, multiple instances of EBOV sexual transmission were reported, including cases where the infectious individual had recovered from EBOV disease months before transmission. Potential human host factors in EBOV sexual transmission remain unstudied. Several basic seminal amyloids, most notably semen-derived enhancer of viral infection (SEVI), enhance in vitro infection by HIV and several other viruses. To test the ability of these peptides to enhance EBOV infection, viruses bearing the EBOV glycoprotein (EboGP) were preincubated with physiological concentrations of SEVI before infection of physiologically relevant cell lines and primary cells. Preincubation with SEVI significantly increased EboGP-mediated infectivity and replication in epithelium- and monocyte-derived cell lines. This enhancement was dependent upon amyloidogenesis and positive charge, and infection results were observed with both viruses carrying EboGP and authentic EBOV as well as with semen. SEVI enhanced binding of virus to cells and markedly increased its subsequent internalization. SEVI also stimulated uptake of a fluid phase marker by macropinocytosis, a critical mechanism by which cells internalize EBOV. We report a previously unrecognized ability of SEVI and semen to significantly alter viral physical properties critical for transmissibility by increasing the stability of EboGP-bearing recombinant viruses during incubation at elevated temperature and providing resistance to desiccation. Given the potential for EBOV sexual transmission to spark new transmission chains, these findings represent an important interrogation of factors potentially important for this EBOV transmission route.

Ebola virus | amyloid | sexual transmission | semen | virus stabilization

The 2014–2016 western Africa Ebola outbreak was the largest Ebola outbreak on record, causing more than 28,652 cases and killing 11,325 (1). Ebola virus (EBOV) disease (EVD) is primarily spread by contact with fluids of an infected individual or body. Months after recovery from EVD, EBOV remains detectable in some individuals, including in semen (2). Cohort studies of male EVD survivors demonstrated that infectious EBOV could be isolated from semen up to 82 d after EBOV onset (3, 4). The maximum recorded persistence of EBOV RNA in semen is 965 d, although the concordance between persistent RNA and infectious virus is unclear (5). During the 2014–2016 EBOV outbreak, multiple cases of sexual transmission—some sparking new transmission chains—were reported in case reports supported by epidemiological and molecular evidence (6–10). Transmission was reported from a male survivor 470 d after his EVD onset (9). An epidemiological model of EBOV sexual transmission in Sierra Leone predicted that even a 3-mo infectious period would extend the length of the outbreak by an average of 83 d (11).

EBOV tropism is broad (12, 13) and histological studies report a wide variety of cell types infected in vivo during infection (12, 14–16). It has been suggested that monocytes, macrophages, and dendritic cells in particular are important early targets for infection (12, 16–19). EBOV entry into cells is enhanced by interactions between the virion and cellular attachment factors, including C-type lectins (e.g., DC-SIGN and DC-SIGNR) (20–24), Tyro3 family members (e.g., Axl) (25), and phosphatidylserine-binding molecule TIM-1 (26). EBOV requires macropinocytosis as an uptake mechanism (27–29), resulting in its trafficking to acidified endosomes where the glycoprotein is processed by cathepsin B/L proteases (30). After processing, the glycoprotein interacts with its receptor Niemann-Pick C1 (NPC1) to effect fusion between the viral and endosomal membranes (31–33).

Screening of protein/peptide libraries derived from human semen identified peptides that dramatically enhance viral infection (34). The most well studied of these is PAP248–286, a highly basic 39-amino acid cleavage product of prostatic acid phosphatase (PAP) (35). While having no impact on HIV-1 infection as a soluble peptide, PAP248–286 assembles into amyloid fibrils termed semen-derived enhancer of viral infection (SEVI) that greatly increase HIV-1 infectivity (35). Subsequent analyses have identified other amyloid fibrils in semen that enhance HIV-1 infection, including another cleavage product of PAP (PAP85–120) (36) and fragments of semenogelin-1 (SEM1) and -2 (SEM2), components of the seminal coagulum (37). Both positive charge and amyloid character are important for enhancement of HIV-1 infection by SEVI, as modified peptides without positive residues form amyloid fibrils with greatly diminished enhancement ability (38). Anionic polymers such as dextran sulfate (38) and molecular tweezers that bind positively charged amino acids (39) inhibit SEVI's enhancement effect, highlighting the importance of charge. Subsequent reports have identified

Significance

During the 2014–2016 Ebola outbreak, multiple instances of male-to-female sexual transmission of Ebola virus (EBOV) were reported. While relatively uncommon, EBOV sexual transmission presents a major public health concern, as these transmission events occurred months after recovery. Further, sexual transmission was linked to a resurgence of EBOV disease in Guinea, which had previously been declared Ebola-free. However, the role of host factors involved in sexual transmission remains unknown. We find that seminal amyloids and semen greatly enhance EBOV infection and alter the virion physical properties, stabilizing viral infectivity and protecting the virus from drying. These results promote seminal amyloids as possible targets for intervention to prevent EBOV sexual transmission and seeding new infection chains that reignite an outbreak.

Author contributions: S.M.B., C.C., J.M.D., J.S., and P.B. designed research; S.M.B. and C.C. performed research; S.M.B., C.C., J.M.D., J.S., and P.B. analyzed data; and S.M.B. and P.B. wrote the paper.

The authors declare no conflict of interest.

This article is a PNAS Direct Submission.

[1]To whom correspondence should be addressed. Email: pbates@pennmedicine.upenn.edu.

This article contains supporting information online at www.pnas.org/lookup/suppl/doi:10.1073/pnas.1721646115/-/DCSupplemental.

enhancement roles for these fibrils for infection by simian immunodeficiency virus, cytomegalovirus, and herpes simplex virus (40–42).

A leading model of SEVI enhancement of infection posits that the highly positive charge of the amyloid fibrils reduces electrostatic repulsion between the negative charges of the virion and cellular membranes. For HIV-1, an increase in virus attachment to the cell surface was detected upon pretreatment of the virus with SEVI relative to virus alone (35). SEVI fibrils are endocytosed by cellular protrusions, but the role this plays in enhancement of viral infection is not known (35).

The ability of sexual transmission to reignite an outbreak warrants examination of factors affecting EBOV sexual transmission. In this study, we addressed whether seminal amyloids enhanced EBOV infection in vitro. Our results indicate that SEVI, other seminal amyloid fibrils, and semen greatly enhanced infection mediated by the EBOV glycoprotein using both nonpathogenic EBOV surrogates and authentic EBOV. This enhanced infection retained requirements for EBOV infection including macropinocytic uptake and cathepsin processing. In addition, we identify a potential role for seminal amyloid fibrils in enhancing viral stability after extended incubation at elevated temperature or upon desiccation.

Materials and Methods

For full materials and methods, please see *SI Appendix*.

Viruses and Cells. Recombinant vesicular stomatitis virus (rVSV) expressing the EBOV glycoprotein and mCherry (rVSV-EboGP-mCherry) has been previously described (43, 44). EBOV/"Zaire 1995" (EBOV/H.sap-tc/COD/95/Kik-9510621) was used in authentic virus studies (45). HeLa, A549, THP1, and Vero CCL81 cell lines and macrophages differentiated from blood monocytes were used for infections. Deidentified seminal plasma was obtained by centrifugation of pooled semen from four donors; seminal plasma filtrate was produced by filtering seminal plasma through an Amicon Ultra 100-kDa cutoff filter unit. Monocytes and semen were collected with informed consent under protocols approved by the University of Pennsylvania Institutional Review Board. Use of primary monocytes and seminal plasma is considered to be a secondary use of deidentified human specimens and are exempt via Title 55 Part 46, Subpart A of 46.101 (b) of the Code of Federal Regulations.

Peptides and Fibrils. SEVI, SEVI-Ala, PAP85–120, SEM1, and SEM2 fibrils were generated by dissolving peptides (Keck Biotechnology Resource Laboratory, Yale University) in PBS, filtering through a 0.2-μm filter, seeding with 1% preformed amyloid, and incubating at 37 °C with shaking at 1,400 rpm (35–37). Amyloid formation was confirmed by assessing thioflavin T fluorescence. Peptide sequences are available in *SI Appendix*, Table S1. α-Synuclein fibrils were provided by Kelvin Luk, University of Pennsylvania, Philadelphia, generated as previously described (46).

Infection Assays. rVSV-EboGP-mCherry was diluted into DMEM-10, supplemented with amyloid fibrils or soluble peptides, and incubated at 37 °C for 15 min. Cells were infected with the mixture and infection was assessed by flow cytometry. Infection by authentic EBOV was done similarly and quantified by automated fluorescence microscopy after immunostaining.

Binding/Internalization Assays. rVSV-EboGP-mCherry was pretreated with or without SEVI, then bound to HeLa cells on ice and either lysed in 1% Triton after 1 h (binding) or warmed to 37 °C for an additional 1 h to allow internalization, then washed, trypsinized, and lysed (internalization). Lysates were analyzed by quantitative Western blotting (Li-Cor) by comparing VSV M signal to GAPDH signal.

Dextran Uptake Assay. HeLa cells were pretreated with different concentrations of SEVI, then incubated with 70 kDa dextran-FITC. Mean fluorescence intensity of internalized FITC was determined by flow cytometry.

Virus Stability Analysis. rVSV-EboGP-mCherry was diluted in artificial semen simulant with or without SEVI fibrils, SEVI-Ala fibrils, or PAP248–286 peptide or alternatively, seminal plasma in PBS. After incubation at 37 °C or room temperature with laminar flow, samples were titered by tissue culture infectious dose 50 ($TCID_{50}$) and normalized to the 0-h time point.

Results

Seminal Amyloids Enhance rVSV-EboGP-mCherry Infection. The enhancement ability of seminal amyloids on EBOV glycoprotein-mediated infection was first assessed with a recombinant vesicular stomatitis virus expressing the EBOV glycoprotein (rVSV-EboGP-mCherry, Fig. 1*A*). Recombinant or pseudotyped VSV systems have been used to explore the interactions of the EBOV glycoprotein and viral membrane with cells during entry due to faithful mimicry of the EBOV infection process in a BSL-2 environment (30, 31, 47, 48). SEVI is the best studied of the seminal amyloids, having been the first characterized and having variants available to explore mechanistic details (35, 38). SEVI amyloid fibrils were assembled from chemically synthesized peptides. After preincubation with SEVI, rVSV-EboGP-mCherry was added to cell lines representing potential target cell types during EBOV sexual transmission, including epithelium-derived HeLa and A549 cells and monocyte-derived THP1 cells. Percent infection was measured by flow cytometry for the mCherry reporter. Preincubation of rVSV-EboGP-mCherry with SEVI resulted in a striking increase in infectivity by 16.9- to 20.5-fold for the cell lines analyzed at 35 μg/mL, the concentration of SEVI reported in human semen (35) (Fig. 1 *B* and *C*). A 4.3-fold increase in output virus titer was observed in primary monocyte-derived macrophages, indicating that the enhancement effect was not limited to cell lines (Fig. 1*D*). These experiments were done at low multiplicity of infection (MOI), when enhancement by SEVI has been characterized as greatest (35). However, due to concerns of reproducibility with such low initial percent infection, most future studies were done at higher MOI, with a concomitant decrease in fold enhancement.

Other amyloidogenic peptides derived from the seminal proteins prostatic acid phosphatase (PAP85–120), SEM1, and SEM2 have been reported to enhance viral infection (36, 37, 41). To determine whether these other amyloid fibrils enhance infection mediated by the EBOV glycoprotein, rVSV-EboGP-mCherry was preincubated with physiological concentrations of SEVI fibrils, PAP85–120 fibrils, representative SEM1 fibrils, or representative SEM2 fibrils at physiological concentrations before infection of HeLa cells (MOI 3). Because of background for these other peptides in the mCherry channel (*SI Appendix*, Fig. S1), infection was quantified by flow cytometry after staining for VSV M protein. We observed that all four amyloid peptides significantly increased infection by rVSV-EboGP-mCherry, with the SEM1 amyloid fibrils exhibiting the highest fold increase of 20.3-fold (Fig. 1*E*). The SEM2 and PAP85–120 peptides also significantly enhanced infection by the recombinant virus by 9.2- and 4.2-fold, respectively. A combinatorial infection using low (5 μg/mL) concentrations of each peptide showed no additional infection beyond that of the greatest fold increase (SEM1) alone, suggesting that under these conditions SEM1 may mask the effects of the other amyloids (*SI Appendix*, Fig. S2). These results demonstrate that rVSV-EboGP-mCherry infection is enhanced by the four amyloid fibrils present in human semen.

SEVI-mediated enhancement of HIV-1 infection is dependent upon the charge and amyloid character of the peptides (35, 38). To determine whether SEVI-mediated enhancement of rVSV-EboGP-mCherry maintains similar requirements, rVSV-EboGP-mCherry was pretreated with equal masses of SEVI fibrils, fibrils in which the positively charged amino acids have been replaced with alanine (SEVI-Ala) (38), or freshly dissolved PAP248–286. HeLa cells were infected with the virus-peptide mixtures (MOI 3) and infection was analyzed by flow cytometry for mCherry expression. Unlike SEVI, which effected a 7.5-fold enhancement of rVSV-EboGP-mCherry infection, infection in the presence of SEVI-Ala- or soluble PAP248–286-treated virus did not differ from rVSV-EboGP-mCherry alone (Fig. 1*F*). These results indicate that like enhancement of HIV-1 infection, positive charge and amyloid character are both critical for rVSV-EboGP-mCherry enhancement.

To confirm that infection is enhanced by endogenous peptides present in semen in addition to chemically synthesized peptides,

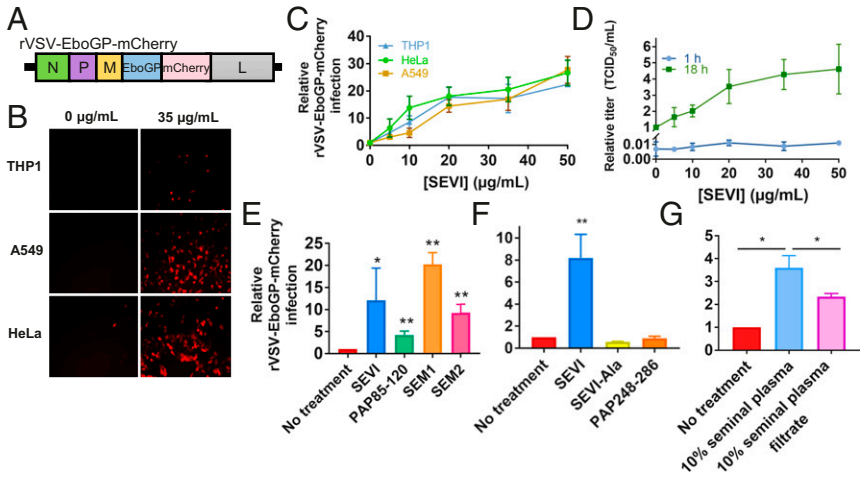

Fig. 1. Seminal amyloids enhance rVSV-EboGP-mCherry infection. (*A*) Genomic organization of rVSV-EboGP-mCherry. (*B*) Fluorescent micrograph of rVSV-EboGP-mCherry infection of HeLa, A549, and THP1 cells (MOI 1) with or without SEVI. (Magnification: 10×.) (*C*) Normalized infection of HeLa, A549, and THP1 cells infected with rVSV-EboGP-mCherry preincubated with SEVI fibrils; $n = 3$, mean ± SEM. (*D*) Normalized output titer of human monocyte-derived macrophages infected with rVSV-EboGP-mCherry (MOI 3) with or without SEVI; $n = 3$, mean ± SEM. (*E*) Normalized infection of HeLa cells infected with rVSV-EboGP-mCherry at MOI 3 with or without 35 μg/mL SEVI fibrils, 39 μg/mL PAP85–120 fibrils, 90 μg/mL SEM1 fibrils, or 90 μg/mL SEM2 fibrils; $n = 3$, mean ± SEM. $^*P < 0.05$, $^{**}P < 0.01$ by ANOVA. (*F*) Normalized infection of HeLa cells infected with rVSV-EboGP-mCherry (MOI 3) pretreated with or without 35 μg/mL SEVI fibrils, SEVI-Ala fibrils, or soluble PAP248–286; $n = 3$, mean ± SEM. $^{**}P < 0.01$ by ANOVA. (*G*) Normalized infection of HeLa cells infected with rVSV-EboGP-mCherry (MOI 3) with 10% seminal plasma or 10% seminal plasma filtrate (cutoff 100 kDa). $n = 3$, mean ± SEM. $^*P < 0.05$ by ANOVA.

rVSV-EboGP-mCherry was incubated with 10% seminal plasma for 5 min before infection of HeLa cells. Low concentrations of seminal plasma must be used to avoid cytotoxic effects (35), although this leads to a concomitant dilution of the amyloids present. A three- to fourfold increase in infectivity was observed under these conditions, an increase which was significantly diminished when the seminal plasma was filtered through a 100-kDa filter unit to remove large molecular weight species such as amyloids (Fig. 1*G*). While this cutoff has been previously used for amyloid studies (49), it may be possible that smaller oligomeric amyloid species may be present and lead to the observed incomplete abrogation of enhancement. These results, however, confirm the ability of semen to enhance infection of a virus bearing the EBOV glycoprotein.

SEVI Enhances EBOV VLP Binding and Internalization. To characterize the mechanism of SEVI-mediated enhancement of EBOV glycoprotein-mediated infection, binding and internalization experiments were performed. rVSV-EboGP-mCherry was preincubated with SEVI before binding to HeLa cells on ice for 1 h. Afterward, the cells were either immediately lysed (binding) or shifted to 37 °C for an additional hour to permit internalization. The internalization cells were then washed, trypsinized to remove bound but uninternalized virus, and lysed. Lysates were analyzed by quantitative Western blotting, and signal in the presence of SEVI was compared with rVSV-EboGP-mCherry binding/internalization in the absence of SEVI. A modest increase in binding (~1.5-fold) was observed in the presence of SEVI at physiological concentrations (Fig. 2*A*). In contrast, the internalization assay demonstrated a linear ($R^2 = 0.9894$) dose-dependent relationship between SEVI preincubation concentration and internalization, with physiological concentrations of SEVI resulting in an ~10-fold increase in internalization of rVSV-EboGP-mCherry after background subtraction (Fig. 2*B*). Further, if rVSV-EboGP-mCherry was bound to HeLa cells on ice in the absence of SEVI, then incubated for 1 h in media containing SEVI, a 10-fold increase in internalization was observed (*SI Appendix*, Fig. S3). This suggests the increase in internalization may, to some extent, be able to occur *in trans* in addition to *in cis*. These findings were further confirmed by binding and internalization assays using EBOV virus-like particles carrying enzymatic or fluorescent reporters (*SI Appendix*, Figs. S4 and S5).

The ability of SEVI to enhance viral internalization has not been previously reported. Previous reports have shown micrographs of SEVI within cells, raising the possibility it may induce endocytosis (35). To explore the ability of SEVI to modulate macropinocytosis in a virus-free environment, HeLa cells were incubated at 37 °C with different concentrations of SEVI for 20 min before the addition of a macropinocytic marker molecule FITC-dextran for 10 min. The cells were treated with PBS pH 4.9 to bleach uninternalized FITC fluorescence, trypsinized, and geometric mean fluorescence intensity (gMFI) was determined by flow cytometry. A linear relationship ($R^2 = 0.9799$) was observed between SEVI concentration and gMFI, with the highest concentrations of SEVI leading to a 3.7-fold increase in macropinocytic uptake (Fig. 2*C*). This increase in fluorescent intensity was ablated in the presence of the macropinocytosis inhibitor 5-(*N*-ethyl-*N*-isopropyl) amiloride (EIPA), indicating efficient bleaching of bound FITC signal and a specificity of macropinocytosis for

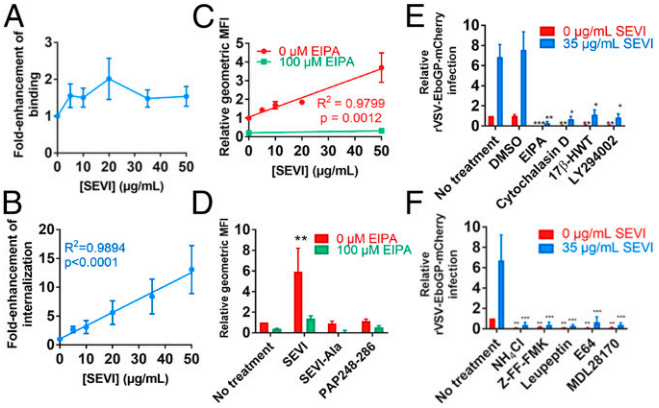

Fig. 2. SEVI enhances rVSV-EboGP-mCherry binding, internalization, and macropinocytosis. (*A*) rVSV-EboGP-mCherry was bound to HeLa cells on ice with or without SEVI fibrils. Cells were lysed and bound virus was quantified by Western blotting; $n = 3$, mean ± SEM. (*B*) rVSV-EboGP-mCherry was bound to HeLa cells on ice with or without SEVI fibrils, then shifted to 37 °C to allow internalization. Cells were washed, trypsinized, and lysed, and internalized virus was quantified by Western blotting; $n = 3$, mean ± SEM. (*C*) HeLa cells were treated with SEVI fibrils, then dextran-FITC in the presence or absence of EIPA. Geometric mean fluorescent intensity was measured by flow cytometry; $n = 3$, mean ± SEM. $^{**}P < 0.01$ by linear regression analysis. (*D*) HeLa cells were treated with or without 35 μg/mL SEVI fibrils, SEVI-Ala fibrils, or soluble PAP248–286, then 70 kDa dextran-FITC. $n = 3$, mean ± SEM. $^{**}P \leq 0.01$ by ANOVA. (*E*) Relative infection of HeLa cells pretreated with macropinocytosis inhibitors and infected with rVSV-EboGP-mCherry (MOI 5) with or without 35 μg/mL SEVI fibrils. (*F*) Normalized percent infection of HeLa cells pretreated with cathepsin inhibitors then infected with rVSV-EboGP-mCherry (MOI 5) pretreated with or without 35 μg/mL SEVI fibrils. (*E* and *F*) $n = 3$, mean ± SEM, $^*P < 0.05$, $^{**}P < 0.01$, $^{***}P < 0.001$ by two-factor repeated measures ANOVA.

uptake (Fig. 2*C*). The enhanced FITC-dextran internalization depended upon the charge and amyloid character of the SEVI peptide, as SEVI-Ala and soluble PAP248–286 peptide treatment showed no increase in dextran uptake (Fig. 2*D*). These results provide evidence for the ability of SEVI to promote macropinocytic uptake to increase internalization of EBOV particles.

SEVI-Mediated Enhancement Maintains EBOV Entry Requirements. Following binding of the virus to the cell, EBOV particles are endocytosed into cells by macropinocytosis and traffic through the endosomal system where cellular cathepsins process the glycoprotein, enabling an interaction of the glycoprotein with its receptor to initiate fusion of the viral and cellular membranes and infection (50). To determine whether the fibril-enhanced infection diverges from the canonical EBOV entry pathway, cells were infected with rVSV-EboGP-mCherry in the presence or absence of inhibitors of macropinocytosis or cathepsin activity, with or without SEVI. No cytotoxic effects were observed with any of these inhibitors (*SI Appendix*, Fig. S6). To inhibit macropinocytosis, HeLa cells were treated with EIPA, cytochalasin D, 17β-hydroxywortmannin (HWT), or LY294002 for 1 h before and 1 h during infection (MOI 5). While infection by rVSV-EboGP-mCherry was enhanced by SEVI in this experiment in the absence of inhibitor, all macropinocytosis inhibitors equally reduced infection by 5- to 10-fold in both the absence and presence of SEVI. These results indicate that macropinocytic entry is not bypassed in the presence of SEVI and that infection maintains this cellular requirement for EBOV glycoprotein-dependent infection (Fig. 2*E*). Similarly, inhibitors of cathepsin activity, including ammonium chloride, E64, Z-FF-FMK, leupeptin, or MDL28170, abrogated infection of HeLa cells by 10- to 20-fold in the presence and absence of physiological levels of SEVI (Fig. 2*F*). These results imply that while SEVI enhances infection, it does not permit the virus to bypass critical cellular requirements for rVSV-EboGP-mCherry entry.

SEVI Alters rVSV-EboGP-mCherry Physical Characteristics. We next hypothesized that seminal amyloid fibrils could affect the physical characteristics of the virus, which may impact transmissibility. To determine if the interaction of viral particles with amyloid fibrils alters the physical characteristics of the virus, we analyzed the effects of thermal and osmotic stresses on viral infectivity. Whether SEVI pretreatment impacts rVSV-EboGP-mCherry stability over time was assessed by incubation of rVSV-EboGP-mCherry with or without physiologic SEVI concentrations in artificial semen simulant (51) for various lengths of time at 37 °C. Artificial semen simulant is designed to mimic the chemical composition of semen and contains 5 mg/mL BSA, making any nonspecific effects of additional protein in the form of peptides to the mixture unlikely. At each time point, the titer of virus was determined by $TCID_{50}$ on Vero cells. Values were normalized to the starting titer for each condition, log transformed, and analyzed by nonlinear regression. Strikingly, the presence of SEVI promoted increased viral viability relative to virus alone ($P = 0.0029$). The normalized titer of virus incubated in the presence of SEVI was ∼17-fold higher than that of virus incubated in semen simulant alone after 36 h (Fig. 3*A*). This enhancement in stability required the positive charge and amyloid character of SEVI, as SEVI-Ala and PAP248–286 had no effect on stability (Fig. 3*A*). Further, addition of SEVI immediately before titration after incubation without SEVI was unable to rescue the effect, suggesting that SEVI exerts its stabilizing effects during the incubation itself independently from its infection enhancement ability (Fig. 3*A*, 0 μg/mL SEVI + 35 μg/mL SEVI). Similar results were observed when rVSV-EboGP-mCherry was incubated with seminal plasma or seminal plasma filtered through a 100-kDa filter to deplete amyloid fibrils. Occurring over a shorter timescale than observed with synthesized peptides in semen simulant, viral stability was enhanced in 10% seminal plasma compared with 10% seminal plasma filtrate (Fig. 3*B*). The increase in stability of ∼3-fold by 12 h was significant ($P = 0.0225$) but likely diminished due to the diluted amyloid concentration in 10% plasma.

Lastly, we assessed whether the presence of SEVI fibrils could improve desiccation tolerance; as enveloped viruses, EBOV and rVSV-EboGP-mCherry are sensitive to drying. rVSV-EboGP-mCherry was diluted in artificial semen simulant in the presence or absence of physiological concentrations of SEVI. Samples were maintained in bulk liquid or spotted into 96-well plates (10 μL) and allowed to air dry. Samples were taken immediately (0 h) or after varying lengths of time drying under laminar flow at room temperature. Dried samples were rehydrated with 200 μL of DMEM and infectivity was quantified by $TCID_{50}$. Samples were also taken at 6 h from bulk liquid kept within a sealed tube to assess independently any effects of incubation at room temperature. $TCID_{50}$/mL measurements were normalized to the initial time point for each and fitted to a plateau-one phase decay model, which reflects the lag in viral decay until after the liquid has evaporated. After 6 h of incubation, the normalized titer of virus desiccated in the presence of SEVI was ∼10-fold higher than in its absence (Fig. 3*C*). Notably, there was no difference in relative viral titer between virus incubated in the presence or absence of SEVI in the bulk liquid protected from desiccation ($P = 0.10$) (*SI Appendix*, Fig. S7). Again, addition of SEVI immediately before titration after desiccation in its absence had no effect on desiccation kinetics (Fig. 3*C*, 0 μg/mL SEVI + 35 μg/mL SEVI). This result indicates that SEVI promotes viral viability after desiccation and rehydration. To better understand the mechanism of SEVI-mediated desiccation tolerance, rVSV-EboGP-mCherry was also incubated with SEVI-Ala and PAP248–286. While the nonamyloid PAP248–286 had no effect on desiccation tolerance, SEVI-Ala unexpectedly increased viral stability to the same extent as SEVI under these conditions. To determine if the presence of any amyloid could have this effect, rVSV-EboGP-mCherry was dried for 6 h in the presence of an equivalent mass of α-synuclein fibrils, which play a role in Parkinson's disease pathogenesis (52). However, no stabilizing effect was seen over incubation in semen simulant alone, suggesting that not all amyloids have this property (*SI Appendix*, Fig. S8). To confirm that this phenomenon occurs in semen as well, rVSV-EboGP-mCherry was diluted into 10% seminal plasma or 10% seminal plasma filtrate and desiccated as

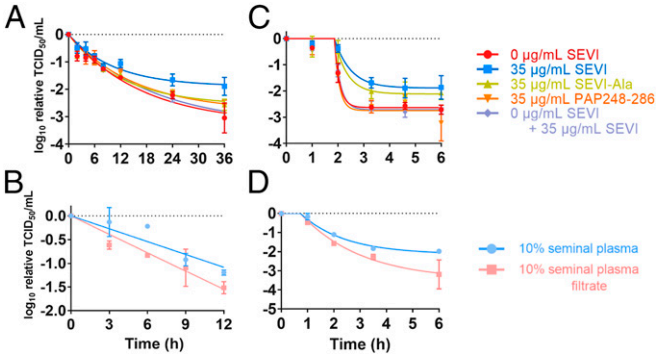

Fig. 3. SEVI alters rVSV-EboGP-mCherry physical characteristics. (*A*) rVSV-EboGP-mCherry was incubated at 37 °C in artificial semen simulant with or without 35 μg/mL SEVI fibrils, SEVI-Ala fibrils, or PAP248–286 peptide and titered by $TCID_{50}$ on Vero cells. In the 0 μg/mL + 35 μg/mL SEVI condition, SEVI was added immediately before titration after incubation without SEVI; $n = 3$, mean ± SEM. (*B*) rVSV-EboGP-mCherry was incubated at 37 °C in 10% seminal plasma or seminal plasma filtrate, then titered by $TCID_{50}$ on Vero cells; $n = 3$, mean ± SEM. (*C*) rVSV-EboGP-mCherry was diluted in artificial semen simulant with or without 35 μg/mL SEVI fibrils and dried under laminar flow before rehydration and titration by $TCID_{50}$ on Vero cells; $n = 3$, mean ± SEM. (*D*) rVSV-EboGP-mCherry was diluted in 10% seminal plasma or seminal plasma filtrate and dried under laminar flow before rehydration and titration by $TCID_{50}$ on Vero cells; $n = 3$, mean ± SEM.

above. A significant decrease in stability ($P = 0.0022$) was observed in the filtrate depleted of amyloid fibrils relative to seminal plasma alone, reaching ~16-fold by 6 h (Fig. 3*D*). Overall, these results indicate a previously unreported ability of seminal amyloid fibrils to stabilize viral infectivity, even after incubation at elevated temperatures over time or desiccation.

Seminal Amyloids Enhance Infection by Authentic EBOV. To confirm that the SEVI enhancement of rVSV-EboGP-mCherry faithfully mimics infection by authentic EBOV, HeLa cells were infected with EBOV after preincubation with various concentrations of SEVI fibrils. Preincubation of EBOV with SEVI led to a dose-dependent enhancement of infection similar to that observed with rVSV-EBOV-mCherry, resulting in a 28.9-fold increase in infection after 24 h at the physiologic concentration of SEVI (MOI 0.2) (Fig. 4*A*). As with EboGP-mediated VSV infection, the EBOV infection enhancement was dependent upon the charge and amyloid nature of the fibrils. In contrast to a 22.8-fold increase in infection observed in the presence of SEVI fibrils in this experiment, EBOV infection (MOI 2) was not enhanced by SEVI-Ala fibrils or soluble PAP248–286 (Fig. 4*B*). Preincubation of EBOV with the other seminal peptides also enhanced infection at 24 h by 37.2-fold for PAP85–120 fibrils, 34.3-fold for SEM1 fibrils, and 41.3-fold for SEM2 fibrils (all 35 μg/mL, MOI 2), in agreement with the results observed for rVSV-EBOV-mCherry (Figs. 1*E* and 4*C*).

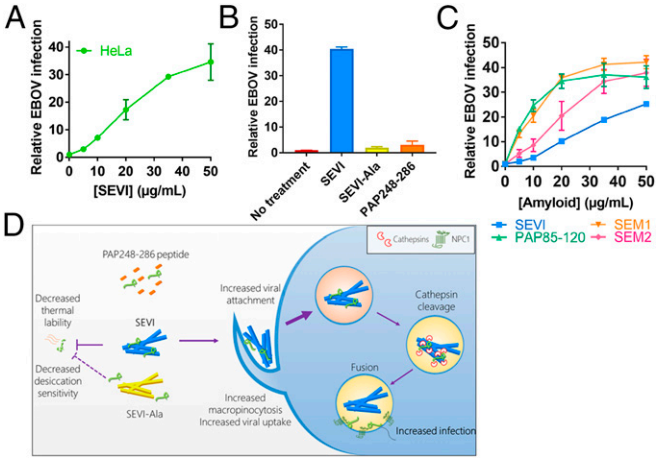

Fig. 4. Seminal amyloids enhance EBOV infection. (*A*) Normalized infection of HeLa cells infected with EBOV (MOI 0.2) preincubated with SEVI fibrils; $n = 2$, mean ± SEM. (*B*) Normalized infection of HeLa cells infected with EBOV (MOI 2) with or without 35 μg/mL SEVI fibrils, SEVI-Ala fibrils, or soluble PAP248–286; $n = 2$, mean ± SEM. (*C*) Normalized infection of HeLa cells infected with EBOV (MOI 2) with SEVI fibrils, PAP85–120 fibrils, SEM1 fibrils, or SEM2 fibrils; $n = 2$, mean ± SEM. (*D*) Model of SEVI-mediated enhancement of EBOV infection.

Discussion

Reports of EBOV sexual transmission during the West Africa Ebola epidemic, although rare, are backed by epidemiological and/or molecular evidence (6–10). Male-to-female transmission of persistent virus has been linked to resurgence of EBOV, but factors potentially involved in EBOV sexual transmission have not been characterized. This report provides evidence that seminal amyloid fibrils, a ubiquitous component of semen in healthy individuals, enhance in vitro infection by both an EBOV surrogate system and authentic EBOV. These fibrils, act in a conformation- and charge-dependent manner to increase infection by increasing virion binding to host cells and enhancing macropinocytotic uptake. We find that these fibrils act to protect virions from stresses encountered during transmission, including thermal degradation and desiccation. We further have replicated these results in seminal plasma containing endogenous seminal amyloids.

Ebola sexual transmission presented a significant and novel public health problem during and following the West Africa Ebola epidemic. Although rare and likely mitigated by public health agencies' safe sex education initiatives, it has become apparent that semen of individuals with persistent EBOV is a potentially important vehicle to consider for EBOV transmission. For a successful male-to-female sexual transmission event, EBOV present in semen must either infect or cross the vaginal epithelium. Recent studies demonstrate that EBOV is able to infect the vaginal epithelium in guinea pig models (53). Notably, the amount of infectious virus in semen has been difficult to determine, but at late time points is likely much lower than that in bodily fluids during acute illness. Prior studies on HIV indicate that the enhancement effect of SEVI is greatest with very low viral inoculums (35); therefore the effect of SEVI may be disproportionately important in EBOV sexual transmission, especially as seminal viral titers wane. Animal models have suggested that macrophages and dendritic cells are early targets of the virus (12, 16–19). Our results indicate that seminal amyloids enhance infection of epithelial and monocytic cells and subsequent viral replication and thus could impact early events in sexual transmission. These cells express numerous attachment factors, including DC-SIGN, which increase the efficiency of infection by EBOV. Whether SEVI permits EBOV to bypass this dependence upon attachment factors or synergistically enhances attachment is not known and worth further study.

In addition, our results demonstrate that amyloids impart resistance of the virus to potentially relevant environmental stresses, including extended incubations at physiological temperatures and desiccation. The ability of environmental factors to affect virion properties and infectivity is seen in other systems. As an example, recent studies have found that bacterial lipopolysaccharide (LPS) induces a conformational change in the poliovirus capsid, increasing virus binding to its cellular receptor and enhancing the stability of the virion under thermal and oxidative stress (54). These data are similar to those we now report on the interaction of an enveloped virus and seminal amyloid fibrils. Unlike the poliovirus and LPS interaction, however, we did not observe an enhancement in rVSV-EboGP-mCherry tolerance to oxidative stress in the presence of SEVI (*SI Appendix*, Fig. S9). After binding to SEVI, rVSV-EboGP-mCherry binding, internalization, and tolerance to environmental stresses increase. The mechanism for this enhanced environmental resistance is unclear, but could involve retention of water molecules by the large amyloid fibrils to create a microenvironment surrounding the virions that is relatively resistant to changes in the larger-scale environment. The exact characteristics necessary for desiccation tolerance are unclear, given the unexpected ability of SEVI and SEVI-Ala to enhance tolerance, while another amyloid did not. Future experiments may involve exploration of the enhancement properties of a wider array of amyloids, as well as testing other viruses such as HIV-1. Resistance to environmental factors may be important to consider when assessing the ability of semen to remain infective over time. Moreover, the seminal amyloids may represent prophylactic drug targets, as strategies to disassemble the amyloids have been investigated (34). Finally, the potential role of amyloid fibrils in viral infection or stability in other physiologic settings such as the gut should be investigated.

Since the identification of seminal amyloid fibrils as enhancers of HIV-1 infection in 2007, infection by several viruses with sexual transmission routes have been found to also be enhanced by SEVI. Mechanistically, enhancement by seminal amyloids has been proposed to enhance binding of the virus to the cell by alleviating repulsive interactions between the viral and cell membranes. Overall, our results suggest a model in which the effect on binding is modest, but that SEVI stimulates macropinocytosis to increase viral internalization in addition to changing the physical properties of the virion (Fig. 4*D*). The enhancement of infection of primary monocyte-derived macrophages as well as the striking increases in macropinocytosis observed in this study are reminiscent of a recent report in which

clearance of sperm cells by macrophages is suggested to be enhanced by seminal amyloids (55). Parallels between the clearance of spermatocytes by macrophages stimulated to engulf the cells by phagocytosis, and internalization of EBOV by phagocytic cells via a similar uptake mechanism are particularly intriguing.

An important limitation of the present study is the inability to study this phenomenon in an in vivo model, as no model for EBOV sexual transmission of persistent virus exists, and the challenges associated with developing one are considerable. However, seminal fibrils may represent an intriguing prophylactic target since agents that affect fibril stability or formation may reduce this increased infectivity at a cellular level as well as enhanced viral stability ex vivo. Altogether, these findings represent analysis of molecular factors potentially involved in EBOV sexual transmission and may promote further study of this transmission route of an important human pathogen.

ACKNOWLEDGMENTS. We thank Valeria Reyes-Ruiz of the Shin laboratory for assistance in the differentiation of primary monocytes; the University of Pennsylvania Human Immunology Core (funding under P30-CA016520) for the primary monocytes; Kurt Barnhart and the Penn Medicine Division of Reproductive Endocrinology and Infertility for seminal plasma samples. We acknowledge funding from T32-AI-007324 (to S.M.B.), Bill and Melinda Gates Foundation Grand Challenges Explorations Award and R21-HD-074510 (to J.S.), Defense Threat Reduction Agency, Project CB10166 (to C.C. and J.M.D.), and Department of Defense Peer Reviewed Medical Research Program Grant W81XWH-14-1-0204 (to P.B.). Disclaimer: Opinions, interpretations, conclusions, and recommendations are those of the authors and are not necessarily endorsed by the US Army.

1. CDC 2014–2016 Ebola Outbreak in West Africa (2016) Ebola Hemorrhagic Fever. Available at https://www.cdc.gov/vhf/ebola/outbreaks/2014-west-africa/index.html. Accessed March 6, 2018.
2. Vetter P, et al. (2016) Ebola virus shedding and transmission: Review of current evidence. *J Infect Dis* 214(Suppl 3):S177–S184.
3. Rowe AK, et al. (1999) Clinical, virologic, and immunologic follow-up of convalescent Ebola hemorrhagic fever patients and their household contacts, Kikwit, Democratic Republic of the Congo. Commission de Lutte contre les Epidémies à Kikwit. *J Infect Dis* 179(Suppl 1):S28–S35.
4. Uyeki TM, et al. (2016) Ebola virus persistence in semen of male survivors. *Clin Infect Dis* 62:1552–1555.
5. Fischer WA, et al. (2017) *Ebola Virus Ribonucleic Acid Detection in Semen More than Two Years After Resolution of Acute Ebola Virus Infection. Open Forum Infectious Diseases* (Oxford Univ Press, Oxford).
6. Mate SE, et al. (2015) Molecular evidence of sexual transmission of Ebola virus. *N Engl J Med* 373:2448–2454.
7. Blackley DJ, et al. (2016) Reduced evolutionary rate in reemerged Ebola virus transmission chains. *Sci Adv* 2:e1600378.
8. Thorson A, Formenty P, Lofthouse C, Broutet N (2016) Systematic review of the literature on viral persistence and sexual transmission from recovered Ebola survivors: Evidence and recommendations. *BMJ Open* 6:e008859.
9. Diallo B, et al. (2016) Resurgence of Ebola virus disease in Guinea linked to a survivor with virus persistence in seminal fluid for more than 500 days. *Clin Infect Dis* 63: 1353–1356.
10. Keita M, et al. (2016) Unusual Ebola virus chain of transmission, Conakry, Guinea, 2014-2015. *Emerg Infect Dis* 22:2149–2152.
11. Abbate JL, Murall CL, Richner H, Althaus CL (2016) Potential impact of sexual transmission on Ebola virus epidemiology: Sierra Leone as a case study. *PLoS Negl Trop Dis* 10:e0004676.
12. Ryabchikova EI, Kolesnikova LV, Luchko SV (1999) An analysis of features of pathogenesis in two animal models of Ebola virus infection. *J Infect Dis* 179(Suppl 1):S199–S202.
13. Wool-Lewis RJ, Bates P (1998) Characterization of Ebola virus entry by using pseudotyped viruses: Identification of receptor-deficient cell lines. *J Virol* 72:3155–3160.
14. Wyers M, et al. (1999) Histopathological and immunohistochemical studies of lesions associated with Ebola virus in a naturally infected chimpanzee. *J Infect Dis* 179(Suppl 1): S54–S59.
15. Connolly BM, et al. (1999) Pathogenesis of experimental Ebola virus infection in Guinea pigs. *J Infect Dis* 179(Suppl 1):S203–S217.
16. Geisbert TW, et al. (2003) Pathogenesis of Ebola hemorrhagic fever in cynomolgus macaques: Evidence that dendritic cells are early and sustained targets of infection. *Am J Pathol* 163:2347–2370.
17. Bray M, Geisbert TW (2005) Ebola virus: The role of macrophages and dendritic cells in the pathogenesis of Ebola hemorrhagic fever. *Int J Biochem Cell Biol* 37:1560–1566.
18. Feldmann H, et al. (1996) Filovirus-induced endothelial leakage triggered by infected monocytes/macrophages. *J Virol* 70:2208–2214.
19. Gupta M, Mahanty S, Ahmed R, Rollin PE (2001) Monocyte-derived human macrophages and peripheral blood mononuclear cells infected with Ebola virus secrete MIP-1alpha and TNF-alpha and inhibit poly-IC-induced IFN-alpha in vitro. *Virology* 284:20–25.
20. Alvarez CP, et al. (2002) C-type lectins DC-SIGN and L-SIGN mediate cellular entry by Ebola virus in cis and in trans. *J Virol* 76:6841–6844.
21. Simmons G, et al. (2003) DC-SIGN and DC-SIGNR bind ebola glycoproteins and enhance infection of macrophages and endothelial cells. *Virology* 305:115–123.
22. Matsuno K, et al. (2010) C-type lectins do not act as functional receptors for filovirus entry into cells. *Biochem Biophys Res Commun* 403:144–148.
23. Powlesland AS, et al. (2008) A novel mechanism for LSECtin binding to Ebola virus surface glycoprotein through truncated glycans. *J Biol Chem* 283:593–602.
24. Takada A, et al. (2004) Human macrophage C-type lectin specific for galactose and N-acetylgalactosamine promotes filovirus entry. *J Virol* 78:2943–2947.
25. Shimojima M, et al. (2006) Tyro3 family-mediated cell entry of Ebola and Marburg viruses. *J Virol* 80:10109–10116.
26. Kondratowicz AS, et al. (2011) T-cell immunoglobulin and mucin domain 1 (TIM-1) is a receptor for Zaire Ebolavirus and Lake Victoria Marburgvirus. *Proc Natl Acad Sci USA* 108:8426–8431.
27. Mulherkar N, Raaben M, de la Torre JC, Whelan SP, Chandran K (2011) The Ebola virus glycoprotein mediates entry via a non-classical dynamin-dependent macropinocytic pathway. *Virology* 419:72–83.
28. Nanbo A, et al. (2010) Ebolavirus is internalized into host cells via macropinocytosis in a viral glycoprotein-dependent manner. *PLoS Pathog* 6:e1001121.
29. Saeed MF, Kolokoltsov AA, Albrecht T, Davey RA (2010) Cellular entry of Ebola virus involves uptake by a macropinocytosis-like mechanism and subsequent trafficking through early and late endosomes. *PLoS Pathog* 6:e1001110.
30. Chandran K, Sullivan NJ, Felbor U, Whelan SP, Cunningham JM (2005) Endosomal proteolysis of the Ebola virus glycoprotein is necessary for infection. *Science* 308:1643–1645.
31. Carette JE, et al. (2011) Ebola virus entry requires the cholesterol transporter Niemann-Pick C1. *Nature* 477:340–343.
32. Côté M, et al. (2011) Small molecule inhibitors reveal Niemann-Pick C1 is essential for Ebola virus infection. *Nature* 477:344–348.
33. Spence JS, Krause TB, Mittler E, Jangra RK, Chandran K (2016) Direct visualization of Ebola virus fusion triggering in the endocytic pathway. *MBio* 7:e01857–e15.
34. Castellano LM, Shorter J (2012) The surprising role of amyloid fibrils in HIV infection. *Biology (Basel)* 1:58–80.
35. Münch J, et al. (2007) Semen-derived amyloid fibrils drastically enhance HIV infection. *Cell* 131:1059–1071.
36. Arnold F, et al. (2012) Naturally occurring fragments from two distinct regions of the prostatic acid phosphatase form amyloidogenic enhancers of HIV infection. *J Virol* 86: 1244–1249.
37. Roan NR, et al. (2011) Peptides released by physiological cleavage of semen coagulum proteins form amyloids that enhance HIV infection. *Cell Host Microbe* 10:541–550.
38. Roan NR, et al. (2009) The cationic properties of SEVI underlie its ability to enhance human immunodeficiency virus infection. *J Virol* 83:73–80.
39. Lump E, et al. (2015) A molecular tweezer antagonizes seminal amyloids and HIV infection. *eLife* 4:e05397.
40. Münch J, et al. (2013) Effect of semen and seminal amyloid on vaginal transmission of simian immunodeficiency virus. *Retrovirology* 10:148.
41. Tang Q, Roan NR, Yamamura Y (2013) Seminal plasma and semen amyloids enhance cytomegalovirus infection in cell culture. *J Virol* 87:12583–12591.
42. Torres L, Ortiz T, Tang Q (2015) Enhancement of herpes simplex virus (HSV) infection by seminal plasma and semen amyloids implicates a new target for the prevention of HSV infection. *Viruses* 7:2057–2073.
43. Jones SM, et al. (2005) Live attenuated recombinant vaccine protects nonhuman primates against Ebola and Marburg viruses. *Nat Med* 11:786–790.
44. Haines KM, Vande Burgt NH, Francica JR, Kaletsky RL, Bates P (2012) Chinese hamster ovary cell lines selected for resistance to ebolavirus glycoprotein mediated infection are defective for NPC1 expression. *Virology* 432:20–28.
45. Jahrling PB, et al. (1999) Evaluation of immune globulin and recombinant interferon-alpha2b for treatment of experimental Ebola virus infections. *J Infect Dis* 179(Suppl 1): S224–S234.
46. Luk KC, et al. (2016) Molecular and biological compatibility with host alpha-synuclein influences fibril pathogenicity. *Cell Rep* 16:3373–3387.
47. Takada A, et al. (1997) A system for functional analysis of Ebola virus glycoprotein. *Proc Natl Acad Sci USA* 94:14764–14769.
48. Lee JE, et al. (2008) Structure of the Ebola virus glycoprotein bound to an antibody from a human survivor. *Nature* 454:177–182.
49. Kim K-A, et al. (2010) Semen-mediated enhancement of HIV infection is donor-dependent and correlates with the levels of SEVI. *Retrovirology* 7:55.
50. Moller-Tank S, Maury W (2015) Ebola virus entry: A curious and complex series of events. *PLoS Pathog* 11:e1004731.
51. Owen DH, Katz DF (2005) A review of the physical and chemical properties of human semen and the formulation of a semen simulant. *J Androl* 26:459–469.
52. Serpell LC, Berriman J, Jakes R, Goedert M, Crowther RA (2000) Fiber diffraction of synthetic alpha-synuclein filaments shows amyloid-like cross-beta conformation. *Proc Natl Acad Sci USA* 97:4897–4902.
53. Cooper TK, et al. (2018) Histology, immunohistochemistry, and in situ hybridization reveal overlooked Ebola virus target tissues in the Ebola virus disease Guinea pig model. *Sci Rep* 8:1250.
54. Robinson CM, Jesudhasan PR, Pfeiffer JK (2014) Bacterial lipopolysaccharide binding enhances virion stability and promotes environmental fitness of an enteric virus. *Cell Host Microbe* 15:36–46.
55. Roan NR, et al. (2017) Semen amyloids participate in spermatozoa selection and clearance. *eLife* 6:e24888.

Supplemental methods

Viruses, cells, and semen. Recombinant VSV expressing the EBOV glycoprotein and mCherry (rVSV-EboGP-mCherry) has been previously described[43,44]. To generate rVSV-EboGP-mCherry stocks, Vero CCL81 cells (gift from Susan Weiss, U. Pennsylvania) were infected at an MOI of 0.001 for 3 days; clarified supernatant was buffered with 25 mM HEPES, aliquoted, frozen at -80°C, and titered by $TCID_{50}$ on Vero CCL81 cells. EBOV/"Zaire 1995" (EBOV/H.sap-tc/COD/95/Kik-9510621) was used in authentic virus studies (1). HeLa, A549, and THP1 cell lines and macrophages differentiated from purified human blood monocytes (UPenn Human Immunology Core) were used as target cells for infections. 293T cells were used for transfection. Seminal plasma was obtained from the Penn Medicine Division of Reproductive Endocrinology and Infertility. Semen was centrifuged at 4000g for 10 min to remove cells, then frozen. To remove amyloid fibrils, seminal plasma was spun through a Amicon Ultra (100 kDa cutoff (2)) for 45 min at 4°C and the filtrate was used; the retentate was discarded. Primary cell and semen samples are considered to be a secondary use of deidentified human specimens and are exempt via Title 55 Part 46, Subpart A of 46.101 (b) of the Code of Federal Regulations. 293T, HeLa, and A549 cells (ATCC) were maintained in DMEM with 4.5 g/L glucose and no sodium pyruvate supplemented with 10% FBS (Sigma). THP1 cells were maintained in RPMI-1640 supplemented with 10% FBS and 50 mM β-mercaptoethanol. Human monocyte-derived macrophages were maintained in RPMI-1640 with glutamine, 10% FBS, and penicillin/streptomycin, and were differentiated from peripheral blood monocytes by incubation in 20 μg/mL MCSF (Gemini) for 7 days.

Peptides and Fibrils. SEVI, SEVI-Ala, PAP85-120, SEM1, and SEM2 fibrils were generated by dissolving peptides (Keck Biotechnology Resource Laboratory, Yale University) in PBS, filtering through a 0.2 μm filter, seeding with 1% preformed amyloid, and incubating at 37°C with shaking

at 1400 rpm. Amyloid formation was confirmed by assessing thioflavin T fluorescence. Aliquots were stored at -80°C and working stocks kept at 4°C. Peptide sequences are available in Supplementary Table 3.1.

Infection assays. rVSV-EboGP-mCherry was diluted into DMEM-10 alone or supplemented with amyloid fibrils or soluble peptides and incubated at 37°C for 15 minutes. 20 μL of the infection mixture was added to each well of target cells in a 96-well plate (plated at 1.5e4 cells/well the previous day in 100 μL DMEM-10) and incubated at 37°C for 1 h, then the media was replaced with fresh DMEM-10 and incubated at 37°C for a total of 12 h. Cells infected in the presence of SEVI were harvested by trypsinization, fixed in 2% paraformaldehyde (PFA), and analyzed by flow cytometry for mCherry expression. For experiments containing amyloids other than SEVI, the cells were fixed, permeablized with 0.1% saponin in FACS buffer (1% BSA, 0.01% sodium azide in PBS), and stained for 1 h with a combination of 1:1000 mouse monoclonal anti-VSV(M) primary antibody (gift from Robert Doms, U. Pennsylvania) and 1:5000 goat anti-mouse secondary antibody labeled with AF488 (Life Technologies) before analysis by flow cytometry. For each experiment, the average of triplicate technical replicates was log-transformed, and transformed percents infection of biological replicates were compared by repeated measures ANOVA with *post hoc* analysis using false discovery rate analysis to correct for multiple comparisons (GraphPad Prism). Monocyte-derived macrophages were treated with B18R (Abcam) for 24 h prior to as well as during infection to inhibit the interferon response.

For authentic virus infections, peptides were diluted to 5-50 μg/ml and pre-incubated with EBOV for 15 minutes. HeLa cells were exposed to peptide/virus inoculum at an MOI of 2.0 or 0.2

PFU/cell for 1 h, after which peptide/virus inoculum was removed and fresh culture media added. At 24-48 h post-infection, cells were formalin-fixed, removed from containment, and immunostained using the 13F6 antibody (3) at 2 μg/ml. Infection was quantified using automated fluorescence microscopy as described (4).

Binding/Internalization assays. rVSV-EboGP-mCherry was pretreated with or without SEVI then bound to HeLa cells on ice. Cells were either lysed in 1% Triton for 10 minutes on ice after 1 h (binding) or warmed to 37°C for 1 h to allow viral internalization, washed 3x in PBS with Ca^{2+} and Mg^{2+}, trypsinized for 10 minutes at 37°C, and lysed with 1% Triton for 10 minutes on ice (internalization). Lysates were separated on a 12% Criterion TGX gel, transferred to nitrocellulose for 1 h, and blocked with TBS Odyssey Blocking Buffer (Li-Cor). Membranes were probed for VSV M (1:1000, Ab as above) and GAPDH (1:2000, rabbit polyclonal, Santa Cruz Biotechnology) in TBS Blocking Buffer/0.2% Tween simultaneously for 1 h, then with IRDye 800CW goat anti-mouse and IRDye 680RD goat anti-rabbit (1:15,000, Li-Cor) in TBS blocking buffer/0.2% Tween. Membranes were then analyzed by quantitative Western blotting by comparing VSV M signal to GAPDH signal for each sample.

Virus-like particle generation. 293T cells were plated in 15 cm plates the day before transfection. Cells were transfected with 7.5 μg each of pCAGGS-EboGP, pCAGGS-VP40, and either pCAGGS-VP40(luc) or pCAGGS-VP40(GFP) with polyethylenimine[48]. Supernatants were collected at 24 and 48 h after transfection, concentrated through a 20% sucrose cushion by ultracentrifugation, resuspended in 1% BSA, 50 mM HEPES-buffered PBS, and frozen at -80°C until use.

VLP binding assay. HeLa cells were plated in a 96-well plate at 1.5e4 cells/well the day before the assay and incubated on ice for 30 min prior to the experiment. SEVI fibrils were diluted to 35 μg/mL in DMEM-10 and mixed with 3 μL concentrated EBOV VLP (VP40-luc) and incubated at 37°C for 10 min. 20 μL of the mixture was added to triplicate wells and spun at 1200g for 30 min at 4°C. After spinning, the cells were washed 5X with cold DMEM-10 and lysed with Bright-Glo luciferase assay buffer (Promega). Luciferase activity was read on a Luminoskan Ascent (Thermo) 10 minutes after addition of assay buffer, and after background subtraction, readings were normalized to 0 μg/mL SEVI condition. Statistical significance was determined by paired t-test of log-transformed data (StataIC 14).

VLP internalization assay. The VLP internalization assay was done similarly to what has been previously described (5). HeLa cells were plated in a 96-well plate at 1.5e4 cells/well the day before the assay. Cells treated with EIPA were pretreated with 100 μM EIPA for 1 h prior to the beginning of the experiment and incubated on ice for 30 minutes prior to the beginning of the experiment. SEVI fibrils were diluted to 35 μg/mL in DMEM-10 and mixed with 2 μL EBOV VLP (VP40-GFP) and incubated at 37°C for 10 min. After incubation, 20 μL of this mixture was added to triplicate wells and spun at 1200g for 30 min at 4°C. The plate was then shifted to 37°C for 1 h. The cells were then trypsinized, fixed in 2% PFA, and analyzed by flow cytometry for geometric mean fluorescence intensity in the GFP channel. Statistical significance was determined by repeated measured ANOVA with false discovery rate correction (GraphPad Prism).

Dextran uptake assay. HeLa cells were plated in a 96-well plate at 1.5e4 cells/well the day before the assay. Cells treated with EIPA were pretreated with 100 μM EIPA for 1 h. Culture medium was removed from each well and replaced with indicated concentrations of SEVI diluted in DMEM-10 with or without 100 μM EIPA in triplicate. The cells were incubated at 37°C for 20

minutes, then 2.5 μL of 20 mg/mL FITC-dextran (70 kDa in DMSO, Invitrogen) was added to each well for 10 minutes at 37°C. Afterward, the medium was removed and replaced with 100 μL of PBS pH 4.9 to bleach any uninternalized FITC. Cells were trypsinized and fixed in 2% PFA, washed 3X with FACS buffer (1% BSA in PBS, 0.1% sodium azide) and analyzed by flow cytometry. Data were analyzed with FlowJo to determine geometric mean fluorescence intensity in the FITC channel. Statistical significance was assessed by linear regression analysis or repeated measures ANOVA with false discovery rate correction (GraphPad Prism).

Inhibitor treatments. HeLa cells were plated in a 96-well plate at 1.5e4 cells/well the day before the assay. Cells treated with inhibitors [100 μM EIPA (Toronto Research Chemicals), 1 μM cytochalasin D (Cayman Chemical Company), 0.5 μM 17-hydroxywortmannin (Cayman Chemical Company), 50 μM LY294002 (Cayman Chemical Company), 50 mM NH_4Cl (Fisher), 10 μM Z-FF-FMK (EMD Biosciences), 10 μM leupeptin (Sigma), 10 μM E64 (EMD Biosciences), or 10 μM MDL28170 (Calbiochem)] were pretreated for 1 h before infection. Cells were infected as described earlier. After 1 h of infection, the virus- and inhibitor-containing medium was removed and replaced with medium without inhibitor for the remainder of the incubation. Infections were harvested and analyzed for percent infection as described above. To test for cytotoxic effects, HeLa cells were treated with inhibitors for 2 h before assessment for viability by the CellTiter 96 AQueous One Solution Cell Proliferation assay kit (Promega) according to manufacturer instructions.

Virus stability analysis. rVSV-EboGP-mCherry was diluted from stock concentrations to concentrations of 1e7 $TCID_{50}$/mL in artificial semen simulant, with or without SEVI fibrils or α-synuclein fibrils (35 μg/mL) or 10% seminal plasma/seminal plasma filtrate. For thermal stability experiments, samples were taken immediately (0 h timepoint) or after indicated times of incubation

at 37°C in a thermocycler with heated lid to minimize evaporation. Samples were frozen at -80°C until titration by $TCID_{50}$. For desiccation tolerance experiments, 10 µL of diluted virus in artificial semen simulant was spotted in the bottom of non-tissue-culture-treated 96-well plates and allowed to dry under laminar flow in a biosafety cabinet at room temperature for indicated lengths of time. For comparison, samples from the bulk liquid (maintained at room temperature in sealed tube) were taken at the initial timepoint and the last timepoint. Samples were immediately titered by $TCID_{50}$ after addition of 200 µL of DMEM to recover virus from the dried samples.

$TCID_{50}$. Vero cells were plated the previous day at 1.5e4 cells/well in 96-well plates. Viral samples were serially diluted in serum-free DMEM then added in 8-fold replicate to 96-well plates. After 48-72 h, wells were scored by presence/absence of viral replication as marked by fluorescent protein expression and cytopathic effects. $TCID_{50}$/mL was calculated by the Spearman & Kärber algorithm (6). Data were log-transformed and analyzed for statistical significance by nonlinear regression (GraphPad Prism).

Supplemental Results

To further confirm these finding, EBOV VLP experiments were performed. Binding was further quantified with a binding assay using EBOV virus-like particles (VLPs). These particles show filamentous morphology and replicate steps of the EBOV entry process (7–10). VLPs with a luciferase reporter were preincubated with SEVI and bound to HeLa cells on ice for 1 h, then the cells were washed, lysed in luciferase assay buffer, and luminescence recorded. In agreement with previous results, an approximately 2-fold increase in binding was observed in the presence of SEVI (Fig S4). VLPs labeled with GFP were preincubated with SEVI and bound to HeLa

cells on ice then shifted to 37°C. After trypsinization, cells were analyzed by flow cytometry for GFP signal. An increase in geometric mean fluorescence intensity of approximately 25% was observed in the presence of SEVI relative to its absence, suggesting that cells internalized a significantly higher quantity of VLPs pretreated with SEVI than not (Fig S5). This effect was ablated by the macropinocytosis inhibitor N-(ethyl-N-isopropyl)-amiloride (EIPA), suggesting efficient removal of bound VLPs from the cell surface.

Supplemental Figure Legends

Figure S1. HeLa cells were treated with seminal amyloids and autofluorescence was measured by flow cytometry. The percentage of cells in the *mCherry* gate indicates background autofluorescence*; shifts in the PAP85-120 and SEM1 populations are readily appreciated*.

Figure S2. HeLa cells were infected with rVSV-EboGP-mCherry with each seminal amyloid alone or together (5 μg/mL each amyloid)

Figure S3. HeLa cells were chilled on ice and rVSV-EboGP-mCherry was bound on ice for 1 h. The media was then removed and replaced with DMEM-10 containing SEVI. The cells were warmed for 1 h at 37°C before washing, trypsinizing, centrifuging, lysing, and finally analyzing the amount of internalized virus by Western blotting for VSV M.

Figure S4. HeLa cells were prechilled and treated with EBOV VLPs (VP40-luc) pretreated with or without 35 μg/mL SEVI fibrils. After spinfection, cell-associated luciferase signal was determined and normalized; n=3, mean ± SEM. **$p<0.01$ by paired t test.

Figure S5. HeLa cells were prechilled and treated with EBOV VLPs (VP40-GFP) pretreated with or without 35 μg/mL SEVI fibrils. After allowing internalization, cells were analyzed for

geometric mean fluorescence intensity of GFP. *p<0.05, ***p<0.001 by repeated measures ANOVA.

Figure S6. HeLa cells were treated for 2 h with inhibitors in concentrations as described in Materials and Methods then cell viability was assessed by the CellTiter 96 AQueous One Solution Cell Proliferation assay. n=2, mean±SD.

Figure S7. rVSV-EboGP-mCherry was diluted in artificial semen simulant alone or supplemented with 35 μg/mL SEVI fibrils and titered either immediately or after six hours of incubation in a sealed tube at room temperature by TCID50 on Vero cells. p=0.10 by paired t test.

Figure S8. rVSV-EboGP-mCherry was incubated in artificial semen simulant under desiccating conditions with or without 35 µg/mL SEVI fibrils and titered by TCID50 on Vero cells. n=1.

Figure S9. rVSV-EboGP-mCherry was diluted in DMEM-10 alone or supplemented with 35 µg/mL SEVI fibrils and treated with PBS or chlorine bleach diluted in PBS for a final concentration of 0.005% hypochlorite for 1 minute. The samples were then neutralized with sodium thiosulfate (10-fold excess of 0.01% solution) and titered by TCID50 on Vero cells. n=1, mean±SD.

Supplemental References

1. Jahrling PB, et al. (1999) Evaluation of immune globulin and recombinant interferon-alpha2b for treatment of experimental Ebola virus infections. *J Infect Dis* 179 Suppl 1:S224-234.
2. Kim K-A, et al. (2010) Semen-mediated enhancement of HIV infection is donor-dependent and correlates with the levels of SEVI. *Retrovirology* 7(1):1–12.
3. Wilson JA, et al. (2000) Epitopes involved in antibody-mediated protection from Ebola virus. *Science* 287(5458):1664–1666.

4. Wec AZ, et al. (2016) A “Trojan horse” bispecific-antibody strategy for broad protection against ebolaviruses. *Science* 354(6310):350–354.

5. Johansen L, et al. (2013) FDA-approved selective estrogen receptor modulators inhibit Ebola virus infection. *Sci Transl Med* 5(190):190ra79.

6. Hierholzer JC, Killington RA (1996) Virus isolation and quantitation. *Virology Methods Manual* (Elsevier), pp 25–46.

7. Noda T, et al. (2002) Ebola virus VP40 drives the formation of virus-like filamentous particles along with GP. *J Virol* 76(10):4855–4865.

8. Kallstrom G, et al. (2005) Analysis of Ebola virus and VLP release using an immunocapture assay. *J Virol Methods* 127(1):1–9.

9. Nanbo A, et al. (2010) Ebolavirus is internalized into host cells via macropinocytosis in a viral glycoprotein-dependent manner. *PLoS Pathog* 6(9):e1001121.

10. Shoemaker CJ, et al. (2013) Multiple cationic amphiphiles induce a Niemann-Pick C phenotype and inhibit Ebola virus entry and infection. *PloS One* 8(2):e56265.

S1

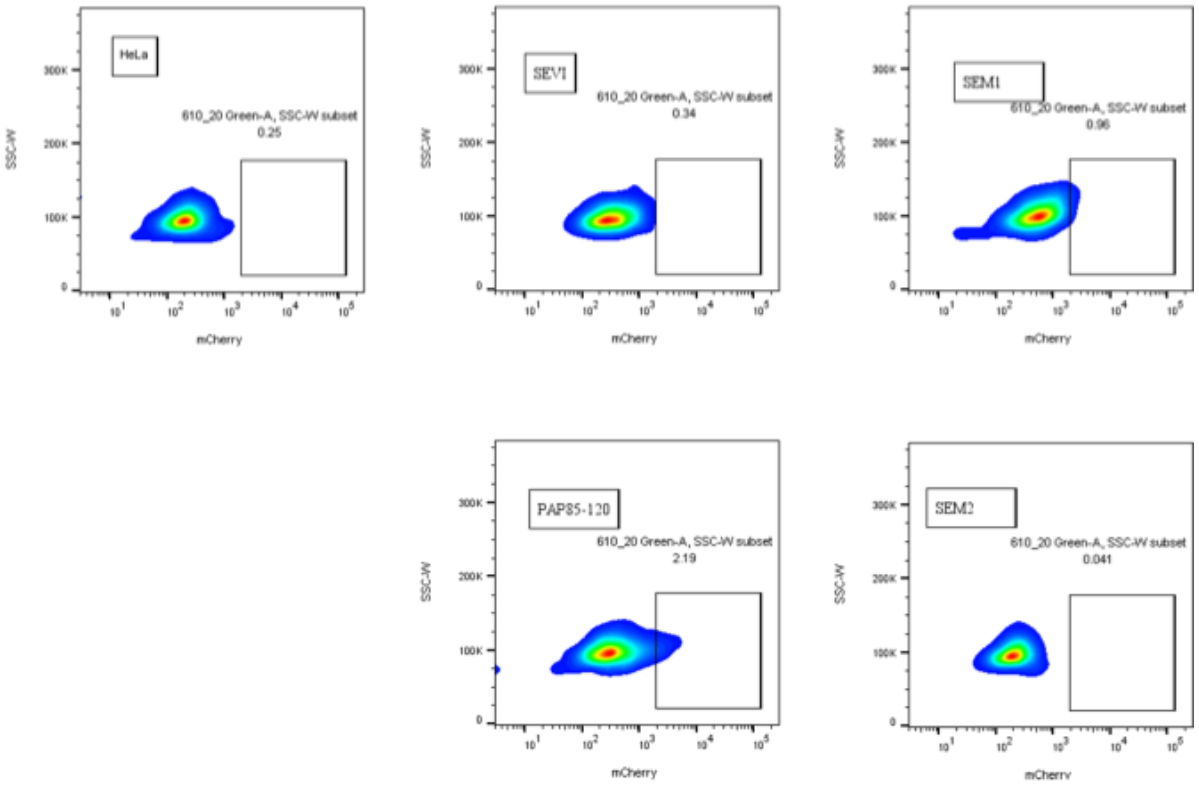
HeLa
610_20 Green-A, SSC-W subset
0.25
SEVI
610_20 Green-A, SSC-W subset
0.34
SEM1
610_20 Green-A, SSC-W subset
0.96
PAP85-120
610_20 Green-A, SSC-W subset
2.19
SEM2
610_20 Green-A, SSC-W subset
0.041
SSC-W
mCherry

S2

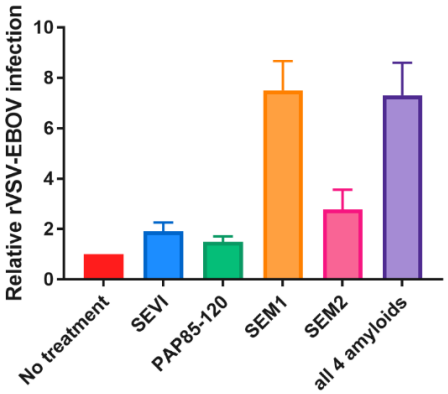
Relative rVSV-EBOV infection
No treatment
SEVI
PAP85-120
SEM1
SEM2
all 4 amyloids

S3

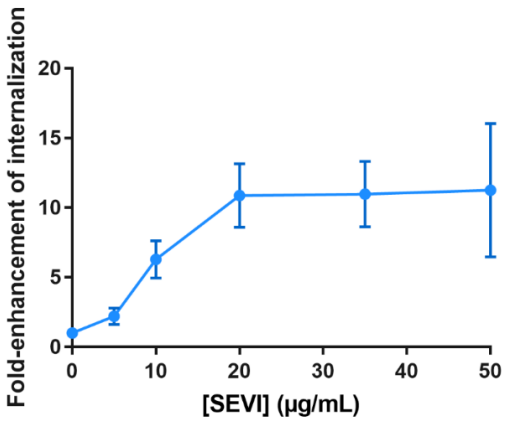
Fold-enhancement of internalization
[SEVI] (µg/mL)

S4

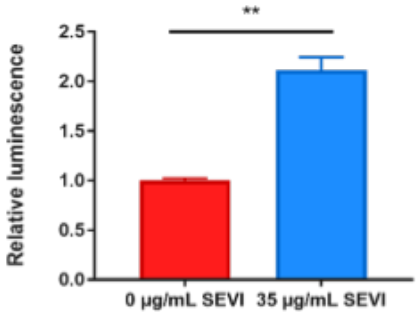
Relative luminescence
0 µg/mL SEVI
35 µg/mL SEVI

S5

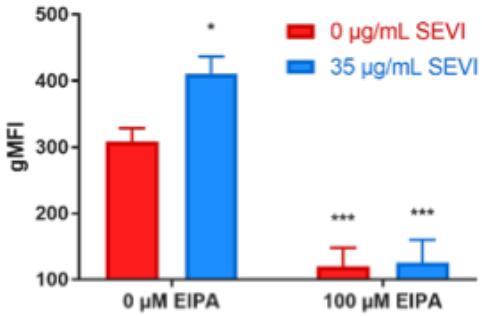
gMFI
0 µg/mL SEVI
35 µg/mL SEVI
0 µM EIPA
100 µM EIPA

S6

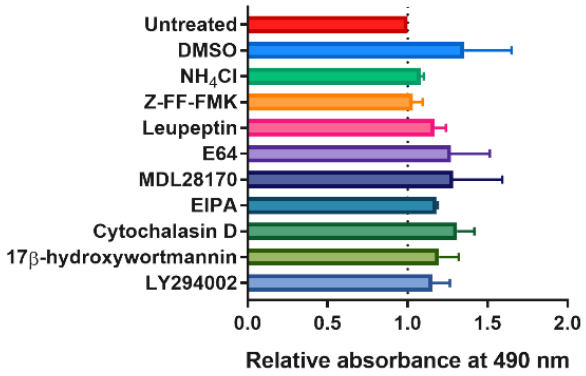
Untreated
DMSO
NH4Cl
Z-FF-FMK
Leupeptin
E64
MDL28170
EIPA
Cytochalasin D
17β-hydroxywortmannin
LY294002
0.0
0.5
1.0
1.5
2.0
Relative absorbance at 490 nm

S7

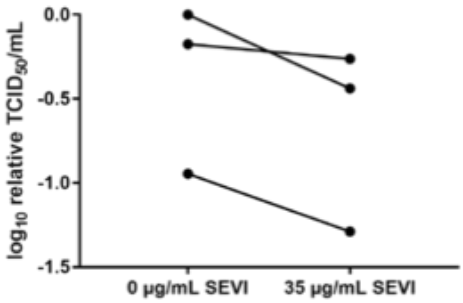
log10 relative TCID50/mL
0.0
-0.5
-1.0
-1.5
0 µg/mL SEVI
35 µg/mL SEVI

S8

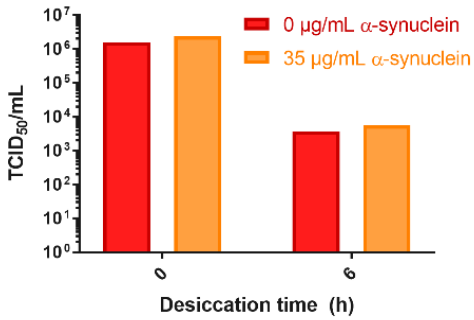
TCID50/mL
0 µg/mL α-synuclein
35 µg/mL α-synuclein
Desiccation time (h)

S9

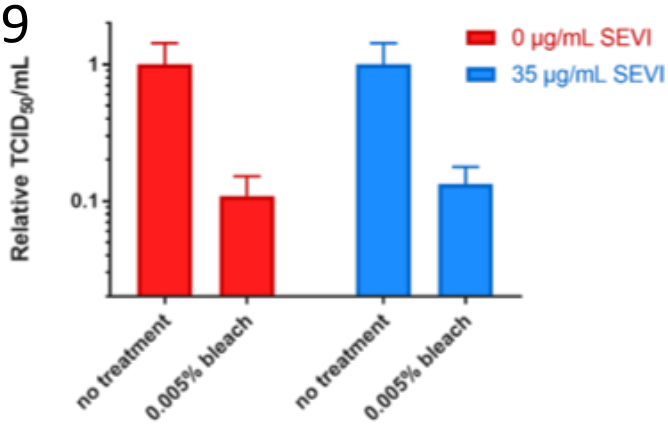
Relative TCID50/mL
0 µg/mL SEVI
35 µg/mL SEVI
1
0.1
no treatment
0.005% bleach
no treatment
0.005% bleach

Supplementary Table 1. Peptide Sequences	
SEVI	GIHKQKEKSRLQGGVLVNEILNHMKRATQIPSYKKLIMY
SEVI-Ala	GIHAQAEASALQGGVLVNEILNHMAAATQIPSYAALIMY
PAP85-120	IRKRYRKFLNESYKHEQVYIRSTDVDRTLMSAMTNL
SEM1 (45–107)	GQHYSGQKGKQQTESKGSFSIQYTYHVDANDHDQSRKSQQYDLNALHKTTKSQRHLGGSQQLL
SEM2 (49-107)	GQKDQQHTKSKGSFSIQHTYHVDINDHDWTRKSQQYDLNALHKATKSKQHLGGSQQLL

Supplementary Table 2. Goodness of fit parameters for Figure 3		
Figure 3A (SEVI-mediated enhancement of stability)		
	R^2	**Overall model p value**
0 µg/mL SEVI	0.9506	0.0007
35 µg/mL SEVI	0.9563	
35 µg/mL SEVI-Ala	0.9665	
35 µg/mL PAP248-286	0.9749	
0 µg/mL SEVI + 35 µg/mL SEVI	0.9689	
Figure 3B (seminal plasma enhancement of stability)		
	R^2	**Overall model p value**
10% seminal plasma	0.8687	0.0003
10% seminal plasma filtrate	0.9533	
Figure 3C (SEVI-mediated enhancement of desiccation tolerance)		
	R^2	**Overall model p value**
0 µg/mL SEVI	0.9821	0.0225
35 µg/mL SEVI	0.9883	
35 µg/mL SEVI-Ala	0.9807	
35 µg/mL PAP248-286	0.9335	
0 µg/mL SEVI + 35 µg/mL SEVI	0.9715	
Figure 3D (seminal plasma enhancement of desiccation tolerance)		
	R^2	**Overall model p value**
10% seminal plasma	0.9884	0.0022
10% seminal plasma filtrate	0.9932	